



OPEN

# Selectivity control in hydrogenation through adaptive catalysis using ruthenium nanoparticles on a CO<sub>2</sub>-responsive support

Alexis Bordet<sup>1,4</sup>, Sami El Sayed<sup>2,4</sup>, Matthew Sanger<sup>3</sup>, Kyle J. Boniface<sup>3</sup>, Deepti Kalsi<sup>1</sup>, Kylie L. Luska<sup>2</sup>, Philip G. Jessop<sup>3</sup> and Walter Leitner<sup>1,2</sup>✉

**With the advent of renewable carbon resources, multifunctional catalysts are becoming essential to hydrogenate selectively biomass-derived substrates and intermediates. However, the development of adaptive catalytic systems, that is, with reversibly adjustable reactivity, able to cope with the intermittence of renewable resources remains a challenge. Here, we report the preparation of a catalytic system designed to respond adaptively to feed gas composition in hydrogenation reactions. Ruthenium nanoparticles immobilized on amine-functionalized polymer-grafted silica act as active and stable catalysts for the hydrogenation of biomass-derived furfural acetone and related substrates. Hydrogenation of the carbonyl group is selectively switched on or off if pure H<sub>2</sub> or a H<sub>2</sub>/CO<sub>2</sub> mixture is used, respectively. The formation of alkylammonium formate species by the catalytic reaction of CO<sub>2</sub> and H<sub>2</sub> at the amine-functionalized support has been identified as the most likely molecular trigger for the selectivity switch. As this reaction is fully reversible, the catalyst performance responds almost in real time to the feed gas composition.**

With the transition from fossil resources to a chemical value chain based on renewable energy and carbon resources, the development of new catalytic technologies to cope with the diversity and variation of feedstock quality is of crucial importance<sup>1–8</sup>. Extensive efforts are currently dedicated to the development of multifunctional catalytic systems able to achieve selective hydrogenation reactions of biomass-derived substrates and intermediates<sup>9–21</sup>. Although many of these catalysts present outstanding properties regarding their dedicated tasks, their performance is typically optimized for static operation under precisely defined parameters. Regional and temporary variations associated with renewable feedstock and energy supply are expected to require a larger degree of process flexibility, however<sup>22,23</sup>. The design and development of catalytic systems whose reactivity can be reversibly adjusted or may even respond adaptively to changes in feedstock composition provide a promising, yet difficult-to-achieve strategy in this context<sup>24</sup>. Known methods to ‘switch’ the reactivity of catalysts typically apply external stimuli, including temperature<sup>25,26</sup>, pH (ref. <sup>27</sup>), solvent variation<sup>24,28</sup>, irradiation<sup>24,28</sup> or redox processes<sup>29–31</sup>. Although these methods are able to generate two different states of a catalyst that exhibit different selectivities, the underlying physical and chemical elementary processes are mostly irreversible or associated with the generation of additional components that accumulate in the reaction mixture. We present here the molecular design of a catalyst that responds with a fully reversible selectivity switch to the presence of CO<sub>2</sub> in the feed gas of a hydrogenation reaction (Fig. 1).

## Results and discussion

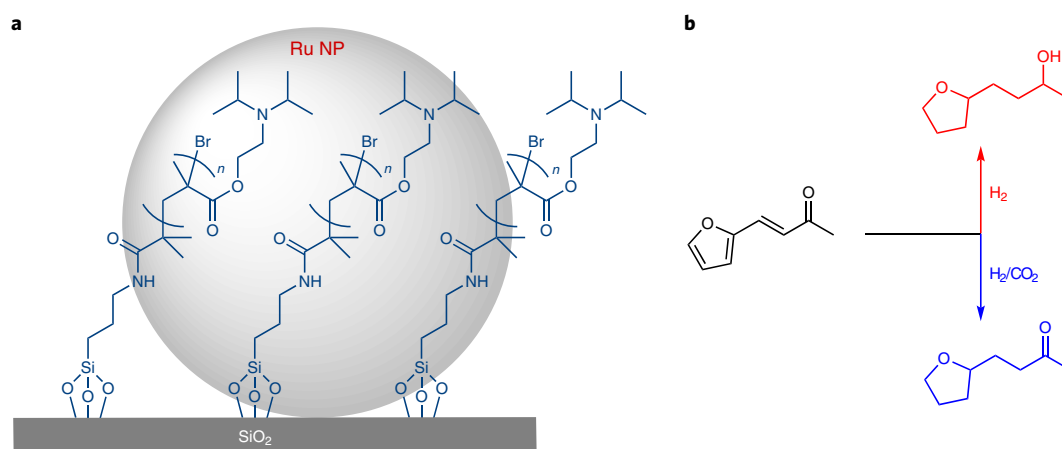
**General strategy.** To enable this adaptivity, a novel bifunctional catalyst was prepared composed of ruthenium nanoparticles (Ru NPs) immobilized on tertiary amine-functionalized polymer-grafted

silica (PGS). The design combined our previous experience of the preparation of Ru NPs for hydrogenation reactions<sup>11,13,15,17</sup> with the use of PGS as a CO<sub>2</sub>-responsive material<sup>32,33</sup>. Furfural acetone (**1**), a biomass-derived platform chemical<sup>34,35</sup>, and similar compounds containing distinct reducible groups were chosen as substrates for hydrogenation in this case study (Fig. 1).

**Synthesis and characterization.** The amine-functionalized PGS was prepared by molecular modification of commercial amorphous SiO<sub>2</sub> particles (Brunauer–Emmett–Teller (BET) surface area = 285 m<sup>2</sup> g<sup>-1</sup>) following a three-step synthetic method previously reported by us involving silanization and surface-initiated atom transfer radical polymerization<sup>32,33</sup>. The synthesis of Ru NPs immobilized on PGS was accomplished using our organometallic approach as a bottom-up synthesis method known to produce small and well-defined Ru NPs on functional supports<sup>17,20</sup>. In brief, metal loading was achieved by wet impregnation of PGS with a solution of [Ru(2-methylallyl)<sub>2</sub>(cod)] (cod, cycloocta-1,5-diene) in dichloromethane. After removal of the solvent in vacuo, the dried powder was subjected to an atmosphere of H<sub>2</sub> (25 bar) at 100 °C for 18 h, giving the desired material, denoted as Ru@PGS (Fig. 1; for synthetic details, see Methods and the Synthesis of Ru@PGS section in the Supplementary Information).

Characterization of Ru@PGS by transmission electron microscopy (TEM; Fig. 2a,b) confirmed the formation of small and well-dispersed Ru NPs (diameter = 1.8 ± 0.4 nm). In addition, elemental mapping using high-angle annular dark-field scanning transmission electron microscopy with energy-dispersive X-ray spectroscopy (HAADF-STEM-EDX; Fig. 2c–g) showed that both the polymer (N and Br mapping, Fig. 2e,f) and the Ru NPs (Ru mapping, Fig. 2g) are homogeneously dispersed on the support

<sup>1</sup>Max Planck Institute for Chemical Energy Conversion, Mülheim an der Ruhr, Germany. <sup>2</sup>Institut für Technische und Makromolekulare Chemie, RWTH Aachen University, Aachen, Germany. <sup>3</sup>Department of Chemistry, Queen's University, Kingston, Ontario, Canada. <sup>4</sup>These authors contributed equally: Alexis Bordet, Sami El Sayed. ✉e-mail: [walter.leitner@cec.mpg.de](mailto:walter.leitner@cec.mpg.de)



**Fig. 1 | General strategy for the CO<sub>2</sub>-switchable hydrogenation of furfural acetone. a**, Structure of the Ru@PGS catalyst composed of Ru NPs immobilized on silica modified with an amine-functionalized polymer. **b**, Model catalytic reaction: the hydrogenation of biomass-derived furfural acetone in the absence or presence of CO<sub>2</sub> in the gas feed.

(Si mapping, Fig. 2d), indicating that they are in close proximity. Rapid decomposition of the organometallic precursor associated with fast nucleation<sup>36</sup> and stabilization by spatial confinement on the SiO<sub>2</sub> support through steric interactions with the polymer chains<sup>37</sup> are presumably important factors for the well-defined particle formation. A Ru loading of 0.82 mmol g<sup>-1</sup> on the PGS (8.2 wt%) was determined using scanning electron microscopy with energy dispersive X-ray spectroscopy (SEM-EDX), consistent with the theoretical value (7.5 wt%). The value obtained from inductively coupled plasma with atom emission spectroscopy (ICP-AES) was a little lower (5.4 wt%), presumably due to the difficulty of fully dissolving the Ru at this relatively high metal loading. The BET surface area of the silica decreased upon polymer grafting from 285 to 55 m<sup>2</sup> g<sup>-1</sup>, and then increased slightly to 84 m<sup>2</sup> g<sup>-1</sup> upon immobilization of the Ru NPs on the support (Supplementary Table 1), consistent with previous reports<sup>38</sup>.

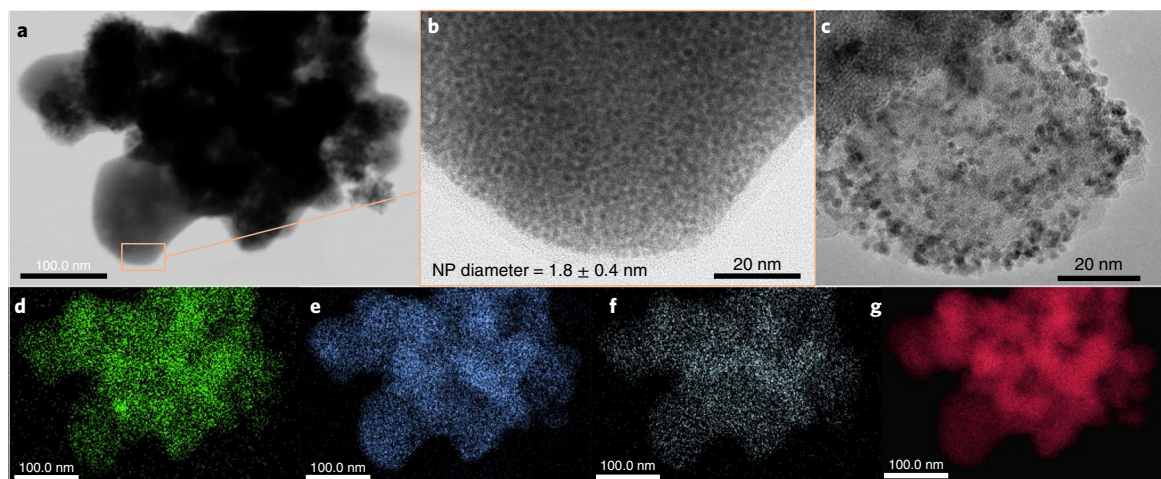
Solid-state <sup>29</sup>Si NMR analysis of the PGS and Ru@PGS showed the presence of tetra- and trifunctionalized Si centres on the polymer-bound SiO<sub>2</sub> surface (Supplementary Fig. 1a,b). The solid-state <sup>13</sup>C NMR spectra of the PGS and Ru@PGS revealed no major differences after the immobilization of the Ru NPs on the support, indicating that the polymer structure is stable under the conditions used for NP synthesis (Supplementary Fig. 1c,d). This is further supported by the fact that the nitrogen content remained unchanged upon Ru NP generation (Supplementary Table 1). In addition, neither [Ru(2-methylallyl)<sub>2</sub>(cod)] nor Ru@PGS showed any activity toward the hydrogenolysis of amide or ester groups in model substrates under these conditions, confirming their inability to cleave the polymer structure (Supplementary Table 2). The amount of accessible amine in the PGS and Ru@PGS was determined to be 1.28 and 1.14 mmol g<sup>-1</sup>, respectively. Thermogravimetric analysis performed under argon showed that the Ru@PGS material starts to lose mass and decomposes at around 200 °C (Supplementary Fig. 2). The material was applied successfully in catalysis at temperatures up to 150 °C, and no signs of decomposition or deactivation were observed at 100 °C for a time on stream of 12 h under continuous-flow conditions (vide infra).

**Catalytic study.** The hydrogenation of furfural acetone (**1**) has been the subject of various studies towards the production of fuel components or chemicals from biomass<sup>3,39,40</sup>. The reaction process starts with C=C bond hydrogenation to form 4-(2-furyl)butan-2-one (**2**). Next, hydrogenation of the furan ring leads to 4-(tetrahydro-2-furyl)butan-2-one (**3**), followed by reduction of

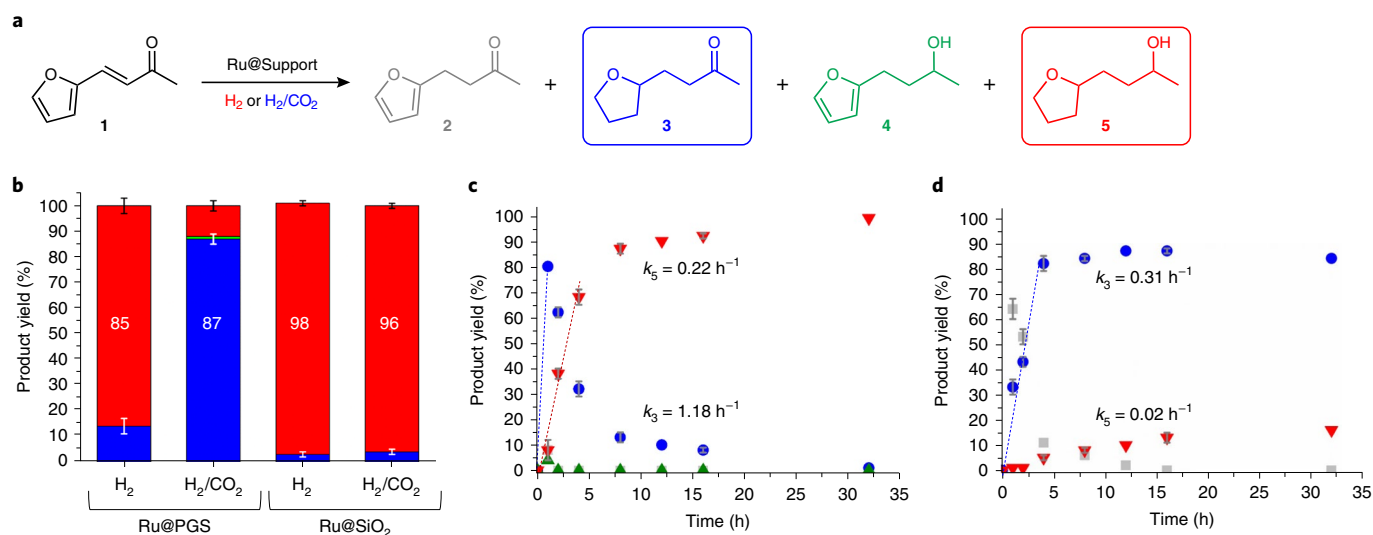
the C=O group to produce 4-(tetrahydro-2-furyl)butan-2-ol (**5**; Fig. 3a). The alternative sequence, with hydrogenation of the ketone in **2** to produce 4-(2-furyl)butan-2-ol (**4**) prior to the reduction of the furan ring, is less preferred over ruthenium catalysts. The presence of several distinct reducible groups thus provides a valuable chemical probe to evaluate the variations in activity and selectivity of hydrogenation catalysts. The catalytic reactions were performed under batch conditions using stainless-steel high-pressure reactors with magnetic stir bars. After parameter screening (Supplementary Table 3), the standard reaction conditions were defined as Ru@PGS (7.5 wt%) with 4 mol% Ru per substrate (1 mol% per reducible group) in butan-1-ol as solvent at *T* = 80 °C for *t* = 16 h. As feed gas, either pure H<sub>2</sub> (15 bar) or a mixture of H<sub>2</sub> and CO<sub>2</sub> (30 bar total pressure, 1:1 ratio) was used to assess the potential influence of CO<sub>2</sub> as a molecular trigger. Using Ru@PGS as catalyst under pure H<sub>2</sub>, furfural acetone (**1**) was hydrogenated to the saturated alcohol **5** in high yield (85%), showing a reactivity typical of Ru NP catalysts<sup>13</sup>.

Varying the total pressure of pure H<sub>2</sub> from 60 to 15 bar did not influence substantially the product distribution (Supplementary Table 3, entries 7 and 13). Applying a mixture of H<sub>2</sub> and CO<sub>2</sub> changed the selectivity drastically, however, leading to the production of the saturated ketone **3** in high yield (87%; Fig. 3b). In sharp contrast, the use of Ru NPs immobilized on non-functionalized SiO<sub>2</sub> as reference (Ru@SiO<sub>2</sub>) resulted in the exclusive formation of **5** (>96% yield) irrespective of the composition of the gas phase. See the 'Synthesis of Ru@SiO<sub>2</sub>' section in the Supplementary Information for synthetic details. Increasing the amount of substrate to 100 equivalents led to the observation of butan-2-ones **2** and **3**, and confirmed the inability of CO<sub>2</sub> to influence the activity and selectivity of Ru@SiO<sub>2</sub> (Supplementary Table 4). For both catalysts under standard conditions, mixing H<sub>2</sub> with Ar gave similar results as under pure H<sub>2</sub>, demonstrating that the simple dilution of H<sub>2</sub> with an inert gas is not sufficient to initiate the selectivity switch (Supplementary Table 5).

The striking effect of the presence of CO<sub>2</sub> on the performance of the Ru@PGS catalyst is evidenced in the product yield–time profiles of the hydrogenation of **1** recorded under H<sub>2</sub> or H<sub>2</sub>/CO<sub>2</sub> atmosphere (Fig. 3c,d and Supplementary Table 6 for the complete data set). With pure H<sub>2</sub>, the hydrogenation of the C=C double bond and the aromatic ring was fast (initial rate constant for the formation of **3**, *k*<sub>3</sub> = 1.18 h<sup>-1</sup>), followed by the hydrogenation of the C=O group with an apparent rate constant of *k*<sub>5</sub> = 0.22 h<sup>-1</sup>. Thus, the fully hydrogenated product **5** was formed in high yield (89%) already after 8 h. In the presence of H<sub>2</sub>/CO<sub>2</sub> the double bond and the furan ring were hydrogenated at somewhat lower rates (*k*<sub>3</sub> = 0.31 h<sup>-1</sup>), producing **3**



**Fig. 2 | Characterization of the Ru@PGS catalyst by electron microscopy.** **a–c**, TEM images of Ru@PGS. The image in **b** is a magnification of the region highlighted by the rectangle in **a**, and **c** shows a magnified image of a different zone of the material. **d–g**, HAADF-STEM-EDX elemental mapping images of Ru@PGS: Si (**d**), N (**e**), Br (**f**) and Ru (**g**). The structure of the catalyst is shown in Fig. 1a. These images show that the Ru@PGS material contains small Ru NPs (diameter =  $1.8 \pm 0.4$  nm) that are well-dispersed over the support. In addition, the grafted polymer covers the silica support homogeneously.



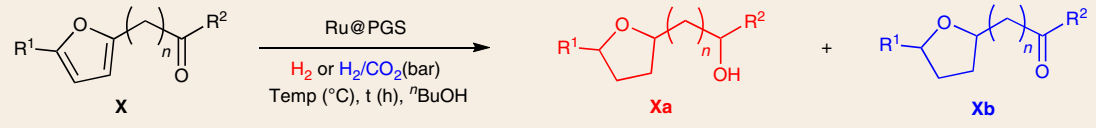
**Fig. 3 | Hydrogenation of furfural acetone (1) under batch conditions.** **a**, Reaction sequence for the hydrogenation of furfural acetone (1). **b**, Product distribution after hydrogenation of furfural acetone (1) under H<sub>2</sub> or H<sub>2</sub>/CO<sub>2</sub> using Ru@PGS or Ru@SiO<sub>2</sub>. Blue represents product 3 and red represents product 5. **c,d**, Reaction time profiles for the hydrogenation of furfural acetone under H<sub>2</sub> (**c**) and H<sub>2</sub>/CO<sub>2</sub> (**d**) using Ru@PGS as catalyst. Grey squares, product 2; blue circles, product 3; green triangles, product 4; red triangles, product 5. Reaction conditions: Ru catalyst (0.026 mmol), substrate (0.65 mmol, 25 equiv.), butan-1-ol (0.5 ml), H<sub>2</sub> (15 bar), H<sub>2</sub>/CO<sub>2</sub> (30 bar, 1:1 ratio), 80 °C, 16 h. The conversion was >99%. The compositions of the reaction mixtures were determined by gas chromatography with flame ionization detection (GC-FID) using tetradecane as internal standard. Experiments were repeated two to four times. Mean values are given and the error bars represent standard deviations. These results show a selectivity switch with the Ru@PGS catalyst when the gas phase composition is changed from pure H<sub>2</sub> to H<sub>2</sub>/CO<sub>2</sub>, with the activity towards C=O hydrogenation becoming very low. In contrast, no influence of the presence of CO<sub>2</sub> was observed when using Ru@SiO<sub>2</sub> as catalyst.

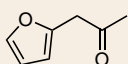
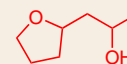
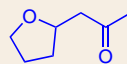
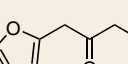

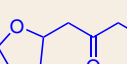
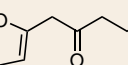
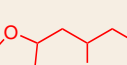
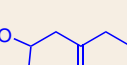
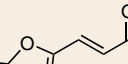
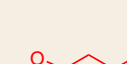
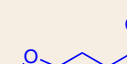
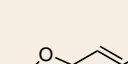

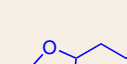
in high yield (84%) after 8 h. Most importantly, C=O hydrogenation was shut down almost completely ( $k_5 = 0.02 \text{ h}^{-1}$ ), leading to less than 20% of 5 even after 35 h reaction time. Between 5 and 20 h of reaction, the ratio of 3 to 5 remained nearly constant at 85:15.

This excellent switch in selectivity, suppressing C=O hydrogenation through the addition of CO<sub>2</sub> to the hydrogen feed gas, was explored under batch conditions using other ketone-containing furan derivatives as substrates. Satisfyingly, the hydrogenation selectivity could be controlled using CO<sub>2</sub> as the molecular trigger for these substrates as well, leading to the selective production

of either saturated alcohols under H<sub>2</sub> or saturated ketones under H<sub>2</sub>/CO<sub>2</sub> under otherwise identical conditions (Table 1).

To investigate molecular changes on the surface of the Ru@PGS catalyst in the presence of carbon dioxide as possible reasons for the drastic reactivity switch, the catalyst was treated with H<sub>2</sub>/CO<sub>2</sub> (30 bar, 1:1) under the standard conditions (80 °C, 16 h) but in absence of any substrate. Deuterated methanol was used as the solvent to allow acquisition of the <sup>1</sup>H and <sup>13</sup>C{<sup>1</sup>H} NMR spectra of the reaction mixture containing the material in suspension. A <sup>13</sup>C signal at 161.5 ppm (Supplementary Fig. 3) indicated the

**Table 1 | Hydrogenation of ketone-containing furan derivatives using Ru@PGS as catalyst under H<sub>2</sub> or H<sub>2</sub>/CO<sub>2</sub>**


Substrate	T °C	t (h)	CO <sub>2</sub> switched OFF		CO <sub>2</sub> switched ON	
			P (H <sub>2</sub> ) (bar)	Main product (% Yield) <sup>a</sup>	P (H <sub>2</sub> /CO <sub>2</sub> ) (bar)	Main product (% Yield) <sup>b</sup>
 <b>6</b>	80	12	15	 <b>6a</b> (99)	15/15	 <b>6b</b> (80)
 <b>7</b>	100	24	30	 <b>7a</b> (90)	30/30	 <b>7b</b> (90)
 <b>8</b>	100	24	30	 <b>8a</b> (70)	30/30	 <b>8b</b> (91)
 <b>9</b>	150	24	40	 <b>9a</b> (70)	40/20	 <b>9b</b> (66)
 <b>10</b>	80	24	15	 <b>10a</b> (95)	15/30	 <b>10b</b> (92)

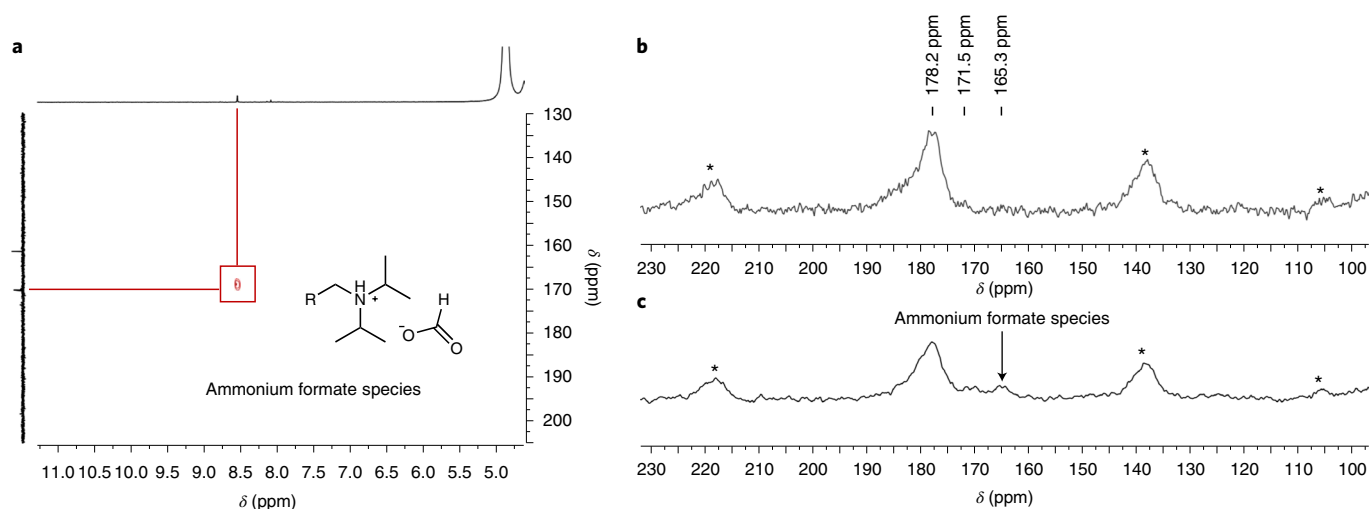
Reactions conditions: Ru@PGS, substrate (25 eq.), butan-1-ol (0.5 mL). Conversion > 99%, product yields were determined by GC-FID using tetradecane as an internal standard. <sup>a</sup>Rest = products **Xb**. <sup>b</sup>Rest = products **Xa**.

presence of an ammonium bicarbonate species, as expected for PGS materials<sup>41,42</sup>. In addition, however, the <sup>1</sup>H and <sup>13</sup>C NMR spectra showed the appearance of strong signals at 8.5 and 169.5 ppm, respectively, which are characteristic of ammonium formate species (Supplementary Figs. 3 and 4)<sup>43,44</sup>. The two-dimensional (2D) heteronuclear single quantum coherence (HSQC) NMR spectrum confirmed the correlation of the two signals (Fig. 4a). Substituting H<sub>2</sub> for D<sub>2</sub> resulted in a 1:1:1 triplet splitting of the <sup>13</sup>C signal at 169.5 ppm, proving that the ammonium formate species is indeed formed by the hydrogenation of CO<sub>2</sub> (Supplementary Fig. 5). Solid-state <sup>13</sup>C cross polarization-magic angle spinning (CP-MAS) NMR analysis of the Ru@PGS material before and after reaction with H<sub>2</sub>/CO<sub>2</sub> revealed a new signal at 165.3 ppm after the reaction, which confirmed the presence of an ammonium formate species also on the spent catalyst (Fig. 4b,c). These data demonstrate that the Ru@PGS catalyst is active in the hydrogenation of CO<sub>2</sub> to formic acid, which is stabilized as ammonium formate species on the amine-decorated support.

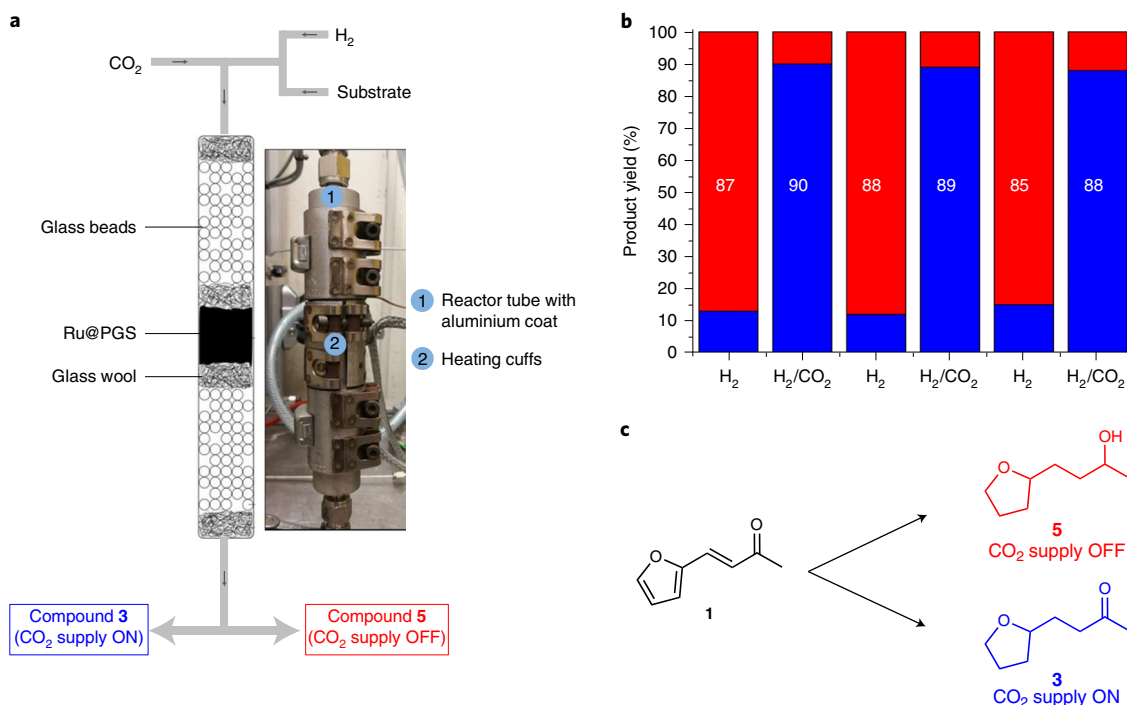
The possible role of formate species in the observed selectivity switch was evaluated through reference experiments using diisopropyl(ethyl)ammonium formate (DIPEF) as a molecular

model for the surface modification (Supplementary Table 7). Adding DIPEF to the catalytic reaction conducted with Ru@PGS as catalyst but with pure H<sub>2</sub> showed a similar suppression of the hydrogenation activity as with H<sub>2</sub>/CO<sub>2</sub>. Most importantly, the addition of DIPEF also steered the hydrogenation of **1** over Ru@SiO<sub>2</sub> selectively towards the ketone **3** (71%, with only 9% of **5**), whereas CO<sub>2</sub> alone had no effect in this case. These data clearly demonstrate that ammonium formate species such as those formed under the H<sub>2</sub>/CO<sub>2</sub> atmosphere on the catalyst surface are able to alter the hydrogenation performance of supported ruthenium particles. Although an additional contribution from the observed bicarbonate species cannot be excluded, we conclude that CO<sub>2</sub> hydrogenation to formate on the catalyst surface plays a key role in the selectivity switch observed under H<sub>2</sub>/CO<sub>2</sub>. One possible hypothesis for this behaviour is that the ammonium formate interacts with the surface of the Ru NPs, preferentially blocking the active sites for the hydrogenation of the more polar C=O group rather than the C=C hydrogenation sites.

As the hydrogenation of CO<sub>2</sub> to formic acid is known to be an equilibrium reaction<sup>45–48</sup>, we evaluated the reversibility of the formate-induced selectivity switch between the formation of **5**



**Fig. 4 | NMR characterization of the Ru@PGS catalyst.** **a**, 2D HSQC NMR (400 MHz, MeOD) spectrum of the Ru@PGS catalyst after reaction with  $H_2/CO_2$ . **b**, Solid-state  $^{13}C$  CP-MAS NMR (125.7 MHz) spectrum before reaction with  $H_2/CO_2$ . **c**, Solid-state  $^{13}C$  CP-MAS NMR (125.7 MHz) spectrum after reaction with  $H_2/CO_2$ , showing the presence of ammonium formate species. The asterisks (\*) indicate spinning side bands. These spectra evidence the formation of ammonium formate species on the catalyst when hydrogenation reactions are performed using  $H_2/CO_2$ .



**Fig. 5 | Switchability tests under continuous-flow conditions.** **a**, Schematic representation and photograph of the continuous-flow set-up. **b**, Hydrogenation of furfural acetone (**1**) using Ru@PGS as catalyst with  $H_2$  and then with  $H_2/CO_2$  (red, product **5**; blue, product **3**). **c**, Selectivity switch controlled by the feed gas composition. Reaction conditions: Ru@PGS (2.0 g, 1.08 mmol), substrate (0.025 M in butan-1-ol, flow rate = 0.5 ml min<sup>-1</sup>, residence time = 6.4 min), 20 bar  $H_2$  or 40 bar  $H_2/CO_2$  (1:1; gas flow rate = 35 ml min<sup>-1</sup>), 100 °C. The conversion was >99%. The compositions of the reaction mixtures were determined by GC-FID using tetradecane as an internal standard. These results demonstrate that the selectivity switch is fully reversible, and that switching back and forth between the gas compositions allows alternating production of the saturated alcohol or ketone in high yields.

versus **3** under batch conditions using the Ru@PGS catalyst in alternating cycles of  $H_2$  and  $H_2/CO_2$  as feed gas. Under the standard conditions, the reactions were found to produce consistently high yields of **5** (73–85%) under  $H_2$  or **3** (84–89%) under  $H_2/CO_2$  in six consecutive runs (Supplementary Fig. 6). Based on these promising results, we implemented the Ru@PGS material in a fully adaptive catalytic system for the hydrogenation of furfural acetone

(**1**). The experiments involved passing a solution of **1** (0.025 M in butan-1-ol) over a packed bed of Ru@PGS (2.0 g) in an in-house built continuous-flow reactor (Fig. 5a and Supplementary Figs. 7 and 8). After screening of the process parameters, the reaction conditions were fixed at 100 °C with a substrate flow of 0.5 ml min<sup>-1</sup> (residence time = 6.4 min) and a gas flow ( $H_2$  or  $H_2/CO_2$ ) of 35 ml min<sup>-1</sup> (Supplementary Table 8). The hydrogenation of furfural acetone (**1**)

was performed for 2 h with pure H<sub>2</sub> (20 bar) before switching to H<sub>2</sub>/CO<sub>2</sub> (40 bar, 1:1) as feed gas for the next 2 h and then back again. Only a short time without substrate delivery was applied between each switch to allow for adjustment of the formate equilibrium (see Methods and the Supplementary Information for details). The feed gas was exchanged five times to evaluate the ability of the catalyst to adapt repeatedly in real time to produce the two different products **3** and **5** under continuous-flow conditions (Fig. 5b).

Under the standard conditions (100 °C, H<sub>2</sub> (20 bar) or H<sub>2</sub>/CO<sub>2</sub> (40 bar, 1:1), substrate flow = 0.5 ml min<sup>-1</sup> (residence time = 6.4 min), 2 h), the reaction changed in a fully reversibly manner to the composition of the feed gas, enabling the system to switch back and forth to produce alternately **5** and **3**, respectively, in high yields (85–90%; Fig. 5b). The selectivity towards the formation of products **3** and **5** could be further improved by optimizing the reaction conditions individually for each production mode (H<sub>2</sub> or H<sub>2</sub>/CO<sub>2</sub>), reaching excellent product yields of 99 and 93% for **3** and **5**, respectively (Supplementary Table 8). TEM characterization of the Ru@PGS material after 12 h on stream did not show notable change in the size and dispersion of the Ru NPs (1.9 ± 0.3 nm; Supplementary Fig. 9). In addition, elemental mapping by HAADF-STEM-EDX evidenced that the polymer and the Ru NPs were still homogeneously distributed over the support (Supplementary Fig. 9e–h). Elemental analysis (SEM-EDX and inductively coupled plasma, ICP) showed that no substantial ruthenium leaching occurred. ICP and BET analysis evidenced a reduced nitrogen content (~30%) and increased surface area (177 m<sup>2</sup> g<sup>-1</sup>), indicating some leaching from the PGS material (Supplementary Table 9). This may be attributed to the loss of non-covalently attached polymer in the early phase of the process, because the performance of the catalyst remained stable throughout the experiment.

## Conclusion

In summary, we have developed a catalytic system that allows a switch in the product selectivity of a hydrogenation reaction with the absence or presence of CO<sub>2</sub> in the feed gas. The design of the catalyst exploited a molecular approach to surface modification and metal nanoparticle formation, depositing Ru NPs by an organometallic approach on amine-functionalized PGS. The key elements are the CO<sub>2</sub>-responsiveness of the surface-attached tertiary amine-functionalized polymer together with the catalytic activity of ruthenium nanoparticles. With the resulting material, the formation of products from the hydrogenation of furfural acetone and other ketone-containing furan derivatives could be controlled to yield selectively either the saturated alcohol or ketone with pure H<sub>2</sub> or H<sub>2</sub>/CO<sub>2</sub>, respectively. As the selectivity switch is induced by the reversible hydrogenation of CO<sub>2</sub>, there is no accumulation of any additional material on the catalyst or in the product stream, allowing waste-free control of the reaction outcome simply by turning on or off the CO<sub>2</sub> supply. In the general context of flexible plant design, this offers potential for two different operating modes without any changes to the catalyst or the reactor unit. The built-in responsiveness would allow the system even to adapt to different feed gas compositions, for example, pure H<sub>2</sub> from water electrolysis or H<sub>2</sub>/CO<sub>2</sub> from biomass reforming.

The formation of alkylammonium formate species at the amine-functionalized support in the presence of CO<sub>2</sub> is believed to play a role in promoting the formation of the ketone over the saturated alcohol, possibly by preferentially blocking the active sites for the hydrogenation of the more polar C=O group rather than the C=C hydrogenation sites. However, the design principle of a CO<sub>2</sub>-responsive surface as support for catalytically active metal nanoparticles or complexes is more generally applicable. We hope that extension of the concept to other metals and other reversible functional groups will open many new opportunities for the development of adaptive catalytic systems to enable flexible production schemes on the basis of renewable feedstock and energy supply.

## Online content

Any methods, additional references, Nature Research reporting summaries, source data, extended data, supplementary information, acknowledgements, peer review information; details of author contributions and competing interests; and statements of data and code availability are available at <https://doi.org/10.1038/s41557-021-00735-w>.

Received: 20 August 2020; Accepted: 18 May 2021;

Published online: 5 July 2021

## References

1. Climent, M. J., Corma, A. & Iborra, S. Conversion of biomass platform molecules into fuel additives and liquid hydrocarbon fuels. *Green Chem.* **16**, 516–547 (2014).
2. Besson, M., Gallezot, P. & Pinel, C. Conversion of biomass into chemicals over metal catalysts. *Chem. Rev.* **114**, 1827–1870 (2014).
3. Leitner, W., Klankermayer, J., Pischinger, S., Pitsch, H. & Kohse-Höinghaus, K. Advanced biofuels and beyond: chemistry solutions for propulsion and production. *Angew. Chem. Int. Ed.* **56**, 5412–5452 (2017).
4. Shylesh, S., Gokhale, A. A., Ho, C. R. & Bell, A. T. Novel strategies for the production of fuels, lubricants, and chemicals from biomass. *Acc. Chem. Res.* **50**, 2589–2597 (2017).
5. Huber, G. W., Iborra, S. & Corma, A. Synthesis of transportation fuels from biomass: chemistry, catalysts, and engineering. *Chem. Rev.* **106**, 4044–4098 (2006).
6. Li, C., Zhao, X., Wang, A., Huber, G. W. & Zhang, T. Catalytic transformation of lignin for the production of chemicals and fuels. *Chem. Rev.* **115**, 11559–11624 (2015).
7. Alonso, D., Bond, J. Q. & Dumesic, J. A. Catalytic conversion of biomass to biofuels. *Green Chem.* **12**, 1493–1513 (2010).
8. Romàn-Leshkov, Y., Barrett, C. J., Liu, Z. Y. & Dumesic, J. A. Production of dimethylfuran for liquid fuels from biomass-derived carbohydrates. *Nature* **447**, 982–985 (2007).
9. Yan, N., Yuan, Y., Dykeman, R., Kou, Y. & Dyson, P. J. Hydrodeoxygenation of lignin-derived phenols into alkanes by using nanoparticle catalysts combined with Brønsted acidic ionic liquids. *Angew. Chem. Int. Ed.* **49**, 5549–5553 (2010).
10. Zhu, Y. et al. Conversion of cellulose to hexitols catalyzed by ionic liquid-stabilized ruthenium nanoparticles and a reversible binding agent. *ChemSusChem* **3**, 67–70 (2010).
11. Luska, K. L., Migowski, P., El Sayed, S. & Leitner, W. Synergistic interaction within bifunctional ruthenium nanoparticle/SILP catalysts for the selective hydrodeoxygenation of phenols. *Angew. Chem. Int. Ed.* **54**, 15750–15755 (2015).
12. Insyani, R., Verma, D., Kim, S. M. & Kim, J. Direct one-pot conversion of monosaccharides into high-yield 2,5-dimethylfuran over a multifunctional Pd/Zr-based metal-organic framework@ sulfonated graphene oxide catalyst. *Green Chem.* **19**, 2482–2490 (2017).
13. Luska, K. L. et al. Enhancing the catalytic properties of ruthenium nanoparticle-SILP catalysts by dilution with iron. *ACS Catal.* **6**, 3719–3726 (2016).
14. Yan, K., Liu, Y., Lu, Y., Chai, J. & Sun, L. Catalytic application of layered double hydroxide-derived catalysts for the conversion of biomass-derived molecules. *Catal. Sci. Technol.* **7**, 1622–1645 (2017).
15. Offner-Marko, L. et al. Bimetallic nanoparticles in supported ionic liquid phases as multifunctional catalysts for the selective hydrodeoxygenation of aromatic substrates. *Angew. Chem. Int. Ed.* **57**, 12721–12726 (2018).
16. Liang, L. et al. Relay catalysis by a multifunctional Cu catalyst in a tandem dehydro-/dehalogenation sequence along with N-arylation. *Org. Lett.* **15**, 2770–2773 (2013).
17. Rengshausen, S. et al. Catalytic hydrogenolysis of substituted diaryl ethers by using ruthenium nanoparticles on an acidic supported ionic liquid phase (Ru@SILP-SO<sub>3</sub>H). *Synlett* **30**, 405–412 (2019).
18. He, R. et al. Tailoring the selectivity of bio-ethanol transformation by tuning the size of gold supported on ZnZr<sub>10</sub>O<sub>x</sub> catalysts. *ChemCatChem* **10**, 3969–3973 (2018).
19. Zhang, F. et al. Mesoporous silica with multiple catalytic functionalities. *Adv. Funct. Mater.* **18**, 3590–3597 (2008).
20. El Sayed, S. et al. Selective hydrogenation of benzofurans using ruthenium nanoparticles in Lewis acid-modified ruthenium-supported ionic liquid phases. *ACS Catal.* **10**, 2124–2130 (2020).
21. Goclik, L., Offner-Marko, L., Bordet, A. & Leitner, W. Selective hydrodeoxygenation of hydroxyacetophenones to ethyl-substituted phenol derivatives using a FeRu@SILP catalyst. *Chem. Commun.* **56**, 9509–9512 (2020).

22. EFFRA *Factories of the Future. Multi-annual Roadmap for the Contractual PPP under Horizon 2020* (European Commission, Luxembourg: Publications Office of the European Union, 2013).
23. *Technology Vision 2020* (The US Chemical Industry, 1996).
24. Blanco, V., Leigh, D. A. & Marcos, V. Artificial switchable catalysts. *Chem. Soc. Rev.* **44**, 5341–5370 (2015).
25. Meng, J. et al. Switchable catalysts used to control Suzuki cross-coupling and aza–Michael addition/asymmetric transfer hydrogenation cascade reactions. *ACS Catal.* **9**, 8693–8701 (2019).
26. Stevens, J. G., Bourne, R. A., Twigg, M. V. & Poliakoff, M. Real-time product switching using a twin catalyst system for the hydrogenation of furfural in supercritical CO<sub>2</sub>. *Angew. Chem. Int. Ed.* **49**, 8856–8859 (2010).
27. Semwal, S. & Choudhury, J. Switch in catalyst state: single bifunctional bi-state catalyst for two different reactions. *Angew. Chem. Int. Ed.* **56**, 5556–5560 (2017).
28. Romanazzi, G., Degennaro, L., Mastrolilli, P. & Luisi, R. Chiral switchable catalysts for dynamic control of enantioselectivity. *ACS Catal.* **7**, 4100–4114 (2017).
29. Lai, A., Hern, Z. C. & Diaconescu, P. L. Switchable ring-opening polymerization by a ferrocene supported aluminum complex. *ChemCatChem* **11**, 4210–4218 (2019).
30. Ibáñez, S., Poyatos, M. & Peris, E. A ferrocenyl-benzo-fused imidazolylidene complex of ruthenium as redox-switchable catalyst for the transfer hydrogenation of ketones and imines. *ChemCatChem* **8**, 3790–3795 (2016).
31. Huang, C. et al. Reversible conversion of valence-tautomeric copper metal–organic frameworks dependent single-crystal-to-single-crystal oxidation/reduction: a redox-switchable catalyst for C–H bonds activation reaction. *Chem. Commun.* **51**, 10353–10356 (2015).
32. Boniface, K. J. et al. CO<sub>2</sub>-switchable drying agents. *Green Chem.* **18**, 208–213 (2016).
33. Boniface, K. J. *CO<sub>2</sub>-Responsive Surfaces*. PhD thesis, Queen's Univ. (2018).
34. West, R. M., Liu, Z. Y., Peter, M. & Dumesic, J. A. Liquid alkanes with targeted molecular weights from biomass-derived carbohydrates. *ChemSusChem* **1**, 417–424 (2008).
35. Subrahmanyam, A. V., Thayumanavan, S. & Huber, G. W. C=C bond formation reactions for biomass-derived molecules. *ChemSusChem* **3**, 1158–1161 (2010).
36. Thanh, N. T. K., Maclean, N. & Mahiddine, S. Mechanisms of nucleation and growth of nanoparticles in solution. *Chem. Rev.* **114**, 7610–7630 (2014).
37. King, S., Hyunh, K. & Tannenbaum, R. Kinetics of nucleation, growth, and stabilization of cobalt oxide nanoclusters. *J. Phys. Chem. B.* **107**, 12097–12104 (2003).
38. Naushad, M., Rajendran, S. & Gracia, F. *Advanced Nanostructured Materials for Environmental Remediation* (Springer, 2019).
39. Dostagir, S. K. N. H. M. D. et al. Selective catalysis for room-temperature hydrogenation of biomass-derived compounds over supported NiPd catalysts in water. *ACS Sustain. Chem. Eng.* **7**, 9352–9359 (2019).
40. Gupta, K. & Singh, S. K. Room-temperature total hydrogenation of biomass-derived furans and furan/acetone aldol adducts over a Ni–Pd alloy catalyst. *ACS Sustain. Chem. Eng.* **6**, 4793–4800 (2018).
41. Lee, J. J. et al. Effect of humidity on the CO<sub>2</sub> adsorption of tertiary amine grafted SBA-15. *J. Phys. Chem. C* **121**, 23480–23487 (2017).
42. Chen, C.-H. et al. The ‘missing’ bicarbonate in CO<sub>2</sub> chemisorption reactions on solid amine sorbents. *J. Am. Chem. Soc.* **140**, 8648–8651 (2018).
43. Wesselbaum, S., Hintermair, U. & Leitner, W. Continuous-flow hydrogenation of carbon dioxide to pure formic acid using an integrated scCO<sub>2</sub> process with immobilized catalyst and base. *Angew. Chem. Int. Ed.* **51**, 8585–8588 (2012).
44. Molinos, B. B. *Carbon Dioxide as C1-Building Block in Combination with Amines: Carbonylation and Hydrogenation Reactions*. PhD thesis, RWTH Aachen Univ. (2015).
45. Jessop, P. G., Ikariya, T. & Noyori, R. Homogeneous hydrogenation of carbon dioxide. *Chem. Rev.* **95**, 259–272 (1995).
46. Leitner, W. Carbon dioxide as a raw material: the synthesis of formic acid and its derivatives from CO<sub>2</sub>. *Angew. Chem. Int. Ed.* **34**, 2207–2221 (1995).
47. Klankermayer, J., Wesselbaum, S., Beydoun, K. & Leitner, W. Selective catalytic synthesis using the combination of carbon dioxide and hydrogen: catalytic chess at the interface of energy and chemistry. *Angew. Chem. Int. Ed.* **55**, 7296–7343 (2016).
48. Sordakis, K. et al. Homogeneous catalysis for sustainable hydrogen storage in formic acid and alcohols. *Chem. Rev.* **118**, 372–433 (2018).

**Publisher's note** Springer Nature remains neutral with regard to jurisdictional claims in published maps and institutional affiliations.



**Open Access** This article is licensed under a Creative Commons Attribution 4.0 International License, which permits use, sharing, adaptation, distribution and reproduction in any medium or format, as long as you give appropriate credit to the original author(s) and the source, provide a link to the Creative Commons license, and indicate if changes were made. The images or other third party material in this article are included in the article's Creative Commons license, unless indicated otherwise in a credit line to the material. If material is not included in the article's Creative Commons license and your intended use is not permitted by statutory regulation or exceeds the permitted use, you will need to obtain permission directly from the copyright holder. To view a copy of this license, visit <http://creativecommons.org/licenses/by/4.0/>.

© The Author(s) 2021

## Methods

**Safety warning.** High-pressure experiments with compressed H<sub>2</sub> must be carried out only with the appropriate equipment and under rigorous safety precautions.

**General.** Unless otherwise stated, the Ru NPs were immobilized on the PGS material (Ru@PGS) under an inert atmosphere (argon) using standard Schlenk techniques or in a glove box. Furfural acetone (**1**) was purified by sublimation prior to use (white crystals). [Ru(2-methylallyl)<sub>2</sub>(cod)] was obtained from Umicore. Synthetic air (20.5 vol% O<sub>2</sub>, the rest N<sub>2</sub>, no hydrocarbon) was purchased from Westfalen. Catalyst solutions and substrates were prepared in air, but were flushed with H<sub>2</sub> and/or CO<sub>2</sub> prior to performing catalytic reactions. All other chemicals and solvents were purchased from commercial sources and used without purification.

**Synthesis of the Ru@PGS catalyst.** [Ru(2-methylallyl)<sub>2</sub>(cod)] (128 mg, 0.401 mmol) was dissolved in DCM (10 ml) and added to a suspension of PGS (500 mg) in DCM (10 ml). The reaction mixture was stirred at room temperature for 1 h. After solvent removal at room temperature and drying the impregnated PGS in vacuo for 1 h, the powder was loaded into a 20-ml high-pressure autoclave and subjected to an atmosphere of H<sub>2</sub> (25 bar) at 100 °C for 18 h. Under this reducing environment, the impregnated PGS transformed from light orange to black, indicating the immobilization of the Ru NPs on the PGS.

**Hydrogenation of furfural acetone (**1**) with H<sub>2</sub>.** The Ru catalyst (35 mg, 0.026 mmol Ru) and butan-1-ol (0.5 ml) were combined with **1** (90 mg, 0.65 mmol, 25 equiv.) in a glass insert and placed in a 10-ml high-pressure autoclave. After purging the autoclave with H<sub>2</sub>, the reaction mixture was stirred at 80 °C in an aluminium heating block under 15 bar H<sub>2</sub>. Once the reaction had finished, the reactor was cooled in an ice bath and carefully vented. After filtration, a sample of the reaction mixture was taken and analysed by GC-FID using tetradecane as internal standard.

**Hydrogenation of furfural acetone (**1**) with CO<sub>2</sub>/H<sub>2</sub>.** The Ru catalyst (35 mg, 0.026 mmol Ru) and butan-1-ol (0.5 ml) were combined with **1** (90 mg, 0.65 mmol, 25 equiv.) in a glass insert and placed in a 10-ml high-pressure autoclave. After purging with CO<sub>2</sub> and stirring for 2 min, the autoclave was further pressurized first with 15 bar CO<sub>2</sub> and then with enough H<sub>2</sub> to raise the total pressure to 30 bar (CO<sub>2</sub>/H<sub>2</sub> ratio ~1:1). The reaction mixture was stirred at 80 °C in an aluminium heating block under the desired pressure of H<sub>2</sub> and CO<sub>2</sub>. Once the reaction had finished, the reactor was cooled in an ice bath and carefully vented. After filtration, a sample of the reaction mixture was taken and analysed by GC-FID using tetradecane as internal standard.

**Hydrogenation of furan derivatives 6–10 with H<sub>2</sub> or CO<sub>2</sub>/H<sub>2</sub>.** Ru@PGS (35 mg, 0.026 mmol Ru) and butan-1-ol (0.5 ml) were combined with the substrate (0.65 mmol, 25 equiv.) in a glass insert and placed in a 10-ml high-pressure autoclave. After purging, the autoclave was pressurized with H<sub>2</sub> (and CO<sub>2</sub>, if applicable) to raise the total pressure to the desired value. The reaction mixture was stirred at the desired temperature in an aluminium heating block. Once the reaction had finished, the reactor was cooled in an ice bath and carefully vented. After filtration, a sample of the reaction mixture was taken and analysed by GC-FID using tetradecane as internal standard.

**Switchability experiments under batch conditions: hydrogenation of furfural acetone (**1**).** The Ru catalyst (35 mg, 0.026 mmol Ru) and butan-1-ol (0.5 ml) were combined with **1** (90 mg, 0.65 mmol, 25 equiv.) in a glass insert and placed in a 10-ml high-pressure autoclave. After purging the autoclave with the respective gases, the reaction mixture was stirred at 80 °C in an aluminium heating block under the desired pressure of the gases used. Once the reaction had finished, the reactor was cooled in an ice bath and carefully vented. The mixture was centrifuged and a sample of the solution was taken and analysed by GC-FID using tetradecane as internal standard. For switchability, the reaction mixture was centrifuged, the supernatant removed and the residue washed with butan-1-ol (3 × 1 ml). The catalyst was then dried at 100 °C for 1 h. For the next cycle, a fresh portion of the substrate (90 mg, 0.65 mmol, 25 equiv.) and butan-1-ol (0.5 ml) were added and the reaction was performed again. This procedure was repeated for each catalytic cycle by alternately pressurizing the autoclave either with only H<sub>2</sub> or with CO<sub>2</sub> and H<sub>2</sub>.

**Hydrogenation of furfural acetone (**1**) in the presence of various additives.** The Ru catalyst (35 mg, 0.026 mmol Ru), butan-1-ol (0.5 ml) and the additive

(0.026 mmol, 1 equiv.) were combined with **1** (90 mg, 0.65 mmol, 25 equiv.) in a glass insert and placed in a 10-ml high-pressure autoclave. After purging the autoclave with H<sub>2</sub>, the reaction mixture was stirred at 80 °C in an aluminium heating block under 15 bar H<sub>2</sub>. Once the reaction had finished, the reactor was cooled in an ice bath and carefully vented. After filtration, a sample of the reaction mixture was taken and analysed by GC-FID using tetradecane as internal standard.

**Switchability experiments in continuous-flow conditions: hydrogenation of furfural acetone (**1**).** The reactor was loaded with the Ru@PGS catalyst (2.0 g, 1.486 mmol Ru, 3.2-ml reactor volume) and installed in the continuous-flow set-up. The system was pressurized with H<sub>2</sub>, heated to the desired temperature and the pump was loaded with the substrate solution. The substrate and gas flows were mixed in a volume flow mixer (alternately H<sub>2</sub> and H<sub>2</sub>/CO<sub>2</sub>), the feed flow was passed through the heated reactor and samples were collected at the output. The compositions of the samples were determined by GC-FID using tetradecane as internal standard. To switch to H<sub>2</sub>/CO<sub>2</sub>, the CO<sub>2</sub> flow was started (35 ml min<sup>-1</sup>), the total pressure at the back-pressure regulator was set to 40 bar and the catalyst was treated for 15 min. The substrate solution flow was then turned on and the first samples were collected after 15 min on stream. To switch to only H<sub>2</sub>, the H<sub>2</sub> and CO<sub>2</sub> flows were turned off, as well as the substrate solution flow. The catalyst was streamed with synthetic air (3 bar) for 1 h at 100 °C, until no solvent was observed at the output. The substrate and H<sub>2</sub> flows were then started again, with the total pressure at the back-pressure regulator set to 20 bar. This procedure was repeated for each switch of atmosphere.

## Data availability

All of the data that support the findings of this study, including material characterizations and catalytic measurements, are available within the paper and its Supplementary Information files (Supplementary Figs. 1–117 and Supplementary Tables 1–9). Further requests about the data can be directed to the corresponding author. Source data are provided with this paper.

## Acknowledgements

The authors acknowledge financial support from the Max Planck Society and from the Deutsche Forschungsgemeinschaft (DFG, German Research Foundation) under Germany's Excellence Strategy – Exzellenzcluster 2186 'The Fuel Science Center' (ID: 390919832). Furthermore, the authors thank N. Avraham (ITMC, RWTH Aachen) for BET absorption measurements, H. Bergstein (ITMC, RWTH Aachen) for ICP-AES measurements, H. Eschmann and E. Biener (ITMC, RWTH Aachen) for GC measurements, M. Emondts (ITMC, RWTH Aachen) for solid-state NMR measurements, N. Pfänder (MPI for Chemical Energy Conversion, Mülheim an der Ruhr), A. Schlüter (MPI for Kohlenforschung, Mülheim an der Ruhr) for TEM analysis, P. Albrecht (ITMC, RWTH Aachen) for his help in the experimental study and C. G. Westhues for his support with the continuous-flow set-up. Scientific discussion with J. Klankermayer is gratefully acknowledged.

## Author contributions

A.B. planned and supervised the experimental work, contributed to the data interpretation and wrote the manuscript. S.E.S. synthesized and characterized the catalysts, performed the catalytic study, interpreted the data and wrote the draft manuscript. M.S. and K.J.B. synthesized the PGS material. D.K. performed the additional experiments required for the revision of the manuscript. K.L.L. supervised part of the experimental work. P.G.J. and W.L. were responsible for the basic project definition and the conceptual planning of experimental work flow. W.L. supervised the project, contributed to the data interpretation and to the writing of the manuscript.

## Competing interests

The authors declare no competing interests.

## Additional information

**Supplementary information** The online version contains supplementary material available at <https://doi.org/10.1038/s41557-021-00735-w>.

**Correspondence and requests for materials** should be addressed to W.L.

**Peer review information** *Nature Chemistry* thanks Jairton Dupont and the other, anonymous, reviewer(s) for their contribution to the peer review of this work.

**Reprints and permissions information** is available at [www.nature.com/reprints](http://www.nature.com/reprints).